Supporting Information

Thompson et al. 10.1073/pnas.0906029106

SI Text

Mapping Details. The aerial photographs for our mapping were taken by Photomap (Kenya) using a Wild RC 10 camera with an 88-mm focal length (super wide angle) lens from flying heights of 7,500 m in 2000 and 2006 and 7,000 m in 2007. Thus, flying heights above Kibo's summit plateau were 1,800 and 1,300 m, resulting in photo scales of ≈1:20,000 and ≈1:15,000, respectively, which, using a conservative estimate of 15 μm for pointing precision on the photographs, yields an expected measurement precision in the terrain of 0.2–0.3 m in plan and 0.3–0.4 m in elevation.

Aerial triangulation resulted in root mean square errors (RMSEs) of residuals at the control points of 3.9 m in easting, 1.3 m in northing, and 8.4 m in elevation for 2000. Subsequently, elevations on the 2000 map were improved by removing a small systematic tilt detected by comparison with results from the Shuttle Radar Topography Mission. RMSEs of residuals at control points in 2006 were 0.7 m in easting, 0.6 m in northing, and 1.1 m in elevation, and in 2007 they were 1.9 m in easting, 0.7 m in northing, and 1.1 m in elevation.

An effort to assess the accuracy of elevation measurements in 2000 was encouraging as the repeatability on a given point with "good" stereo viewing agreed very well with the expected value. On the very smooth February 2000 surface of the FWG the standard deviation was ≈2½ times greater. Similar results are to be expected with similar ice surface conditions.

Areal Coverage Determinations by Cullen et al. (1) and Thompson et al. (2). Cullen et al. (1) used Quickbird satellite imagery from 2003 and calculated the ice cover as 2.51 km^2. They suggested that Thompson et al. (2) had omitted a number of small ice bodies in their 2000 compilation. The slight discrepancy (0.29 km^2) in total ice cover between the Cullen et al. (1), henceforth CU06, ice area and the Ohio State University figure of 2.22 km^2 interpolated from our 2000 and 2006 maps (henceforth OSU-Int) arises primarily from differing interpretations of what is ice and what is transient snow, particularly on the mountain's slopes (1, 2). This minor difference does not affect our conclusions, but it is important to document the origin of the difference as it highlights the difficulties often encountered when using aerial photography or satellite imagery to evaluate ice cover and distinguish what is transient snow and what is ice. A detailed discussion of each domain and its ice entities present in the different aerial photographs is posted on our web site (http://bprc.osu.edu/Icecore/KilimanjaroGlacierRetreat.html). Only the major differences and a few examples are highlighted here. The coding for glacier entities is given in Hastenrath and Greischar (3), reiterated by Thompson et al. (2) and Cullen et al. (1), and is also used here (Fig. S2).

Only four of the seven ice field domains defined by Hastenrath and Greischer (figure 2 in ref. 3) remain (A, D, E and F). Domain A consists of the NIF, the Eastern Ice Field, and the LP and Uhlig glaciers; domains D and E are on the southern slopes; and domain F is the FWG (Fig. S2). To compare Ohio State University ice cover measurements with those in CU06, we determined the area of ice on Kilimanjaro for the February 1, 2003 epoch of CU06 by linear interpolation between the areas in 2000 (figure 1*a* in ref. 1) and 2006 (Fig. S1 and Table S1). The total area (OSU-Int) is 2.224 km^2 and similarly interpolated values for the individual domains are given in Table S2 along with the values of CU06.

There is very good agreement for areas on the plateau. For domain A the agreement is within 0.4%, and there is no difference for domain F. Therefore, the discrepancy in the total ice area is caused by differences on the southern slopes of the mountain (domains D and E), specifically where CU06 have classified certain entities as ice that we considered to be transient snow. The small differences between the measurements of the glaciers on the plateau of Kibo (domains A and F) imply that the differences on the southern slope are not caused by errors in measurements of the ice margins once their locations have been determined, but rather to differences in distinguishing ice from transient snow.

Many of the additional features identified by CU06 as ice entities look like snow in the 2000 photographs in our opinion and are entirely absent in 2006. For example, entity 14 (Fig. S3) looks clearly like snow in 2000 and is entirely absent in 2006. The "small body of ice above the Arrow Glacier" has been interpreted as a snow bank because of its shape and very smooth surface. Examination of this region in the 2007 photographs is inconclusive but observations on the ground show that there is some ice there. This region is obscured by shadows in all of the photographs, which makes interpretation particularly difficult. Because of the azimuth and elevation of the sun at the time the Quickbird image was acquired, it is probably in shadow on it as well. Finally, the "lower ice lobe of the Diamond Glacier" appears to be snow with rock ridges protruding in many places in both 1962 and 2000. There are only a few small scattered patches of snow among very steep-walled rocks in 2006. For additional similar examples of interpretative discrepancies see http://bprc.osu.edu/Icecore/KilimanjaroGlacierRetreat.html.

Another reason for the discrepancy is that the 1912 outline of domain D in CU06 (figure 1 in ref. 1) does not agree with the outline of Hastenrath and Greischar (figure 4 in ref. 3) on which they say it is based. This is evident in Fig. S4. Hastenrath and Greischar's (3) outlines for 1976 and 1989 are based on satellite images of relatively coarse resolution (80 m for Landsat 2 MSS in 1976 and 30 m for Landsat 4 TM in 1989) but it appears that the omission of these two small areas is not caused by the low resolution of their images because the Uhlig Glacier (no. 15), which is approximately the same size as entity 14, is outlined for both epochs. The Great Breach Glacier (no. 12) is present only through 1976 and is in the same location as in the United Nations Environmental Programme/Division of Early Warning and Assessment poster of 2001 (www.unep.org/dewa/assessments/EcoSystems/land/mountain/VanKilimanjaro/index.asp). An unidentified patch of ice that appears to be approximately in the location of CU06's lower ice lobe of the Diamond Glacier is shown only through 1953. Interestingly, the Diamond Glacier (no. 10) is shown only through 1976.

Discussion of the Volume Calculation. As illustrated in Fig. S5*A* our calculation of the total volume loss overestimates the loss caused by thinning (entity 1) and underestimates caused by shrinking (entity 2). Fig. S5*B* illustrates that the volume of entity 3 is lost by a combination of shrinking and thinning. Because no additional information is available it seems appropriate to approximate the retreat from the upper ice edge in 2000 to that in 2007 as shown by the arrow that bisects entity 3 such that the area of entity 3_t equals that of entity 3_r. When multiplied by the surface lowering (ΔT) the best estimate of the volume loss caused by thinning (V_t) is equal to the volume of entity 1 minus entity 3_r (Fig. S5*B*) and that caused by shrinking is equal to the volume of entity 2 + entity 3_r. The calculations are shown in Table S3.

1. Cullen, NJ, et al. (2006). Kilimanjaro Glaciers: Recent areal extent from satellite data and new interpretation of observed 20th-century retreat rates. *Geophys Res Lett*, 10.1029/2006GL027084.
2. Thompson LG, et al. (2002) Kilimanjaro ice core records: Evidence of Holocene climate change in tropical Africa. *Science* 298:589–593.
3. Hastenrath S, Greischar L (1997) Glacier recession on Kilimanjaro, East Africa, 1912–1989. *J Glaciol* 43:455–459.

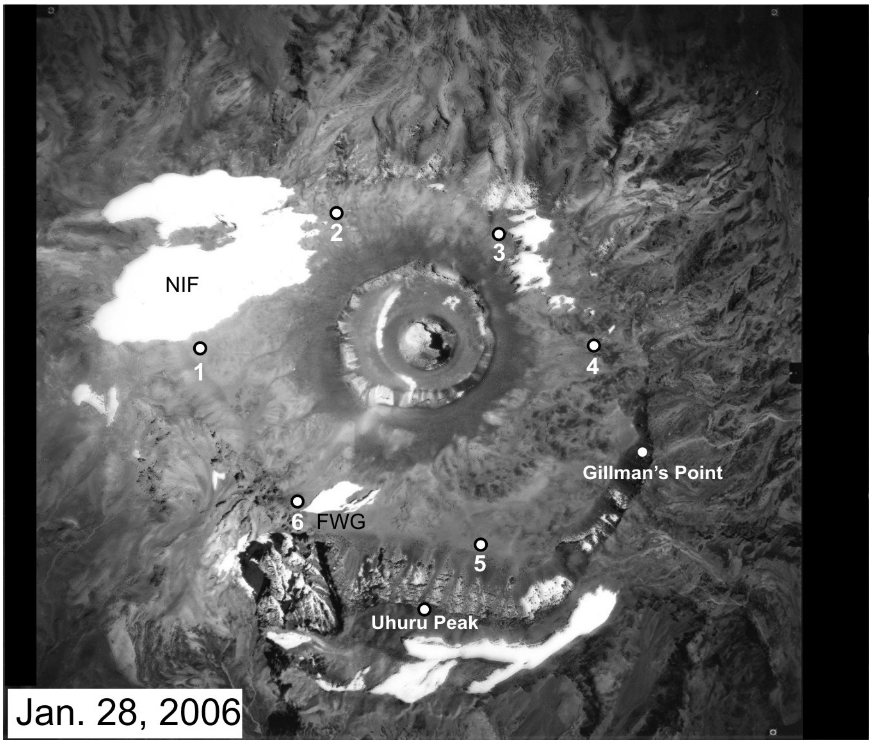

Fig. S1. Aerial photograph of the ice fields atop Kilimanjaro on January 28, 2006.

Total Area Of Ice On Kilimanjaro (1912, 1953, 1976, 1989, 2000, 2007)

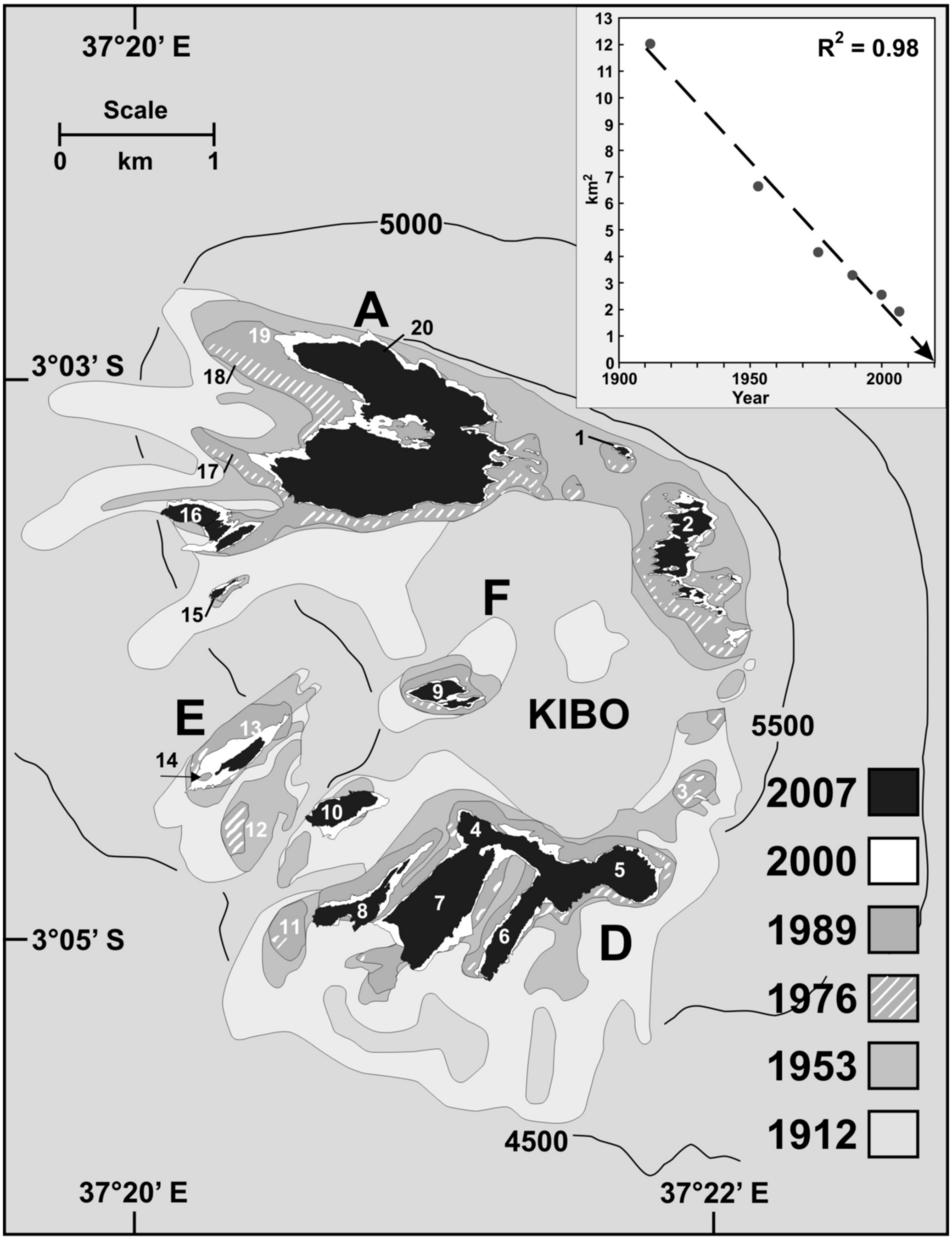

Maps for 1912 - 1989, domains (A, D, E, F) and glaciers 1 - 20 after Hastenrath and Greischar, *J. Glaciol.*, 1997; 2000 after Thompson *et al.*, *Science*, 2002

Fig. S2. Map of Kilimanjaro ice fields (Fig. 2) modified by adding the domains and numbered ice fields according to the classification by Hastenrath and Greischar (3).

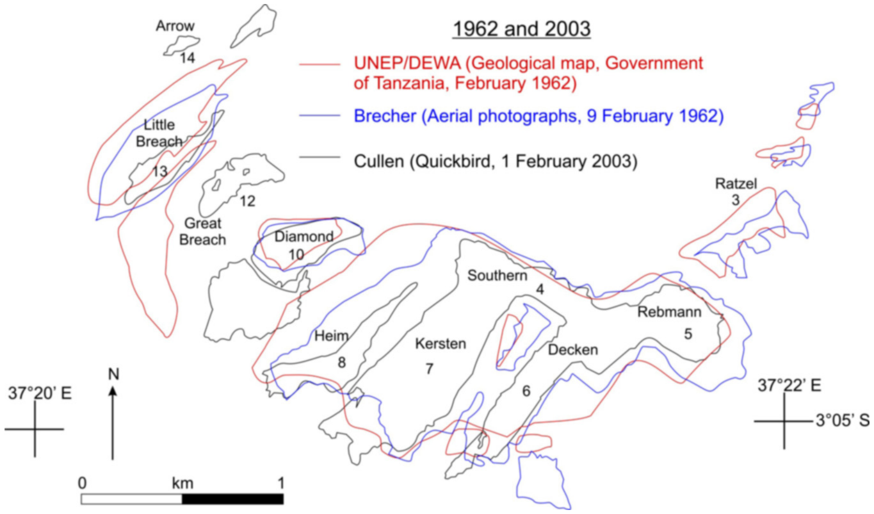

Fig. S3. Comparison of the glacier outlines in domains D and E by Cullen (1) for 2003, by the United Nations Environmental Programme/Division of Early Warning and Assessment 2001 (www.unep.org/dewa/assessments/EcoSystems/land/mountain/VanKilimanjaro/index.asp), and by H.H.B. (this paper) for 1962 (also see http://bprc.osu.edu/Icecore/KilimanjaroGlacierRetreat.html).

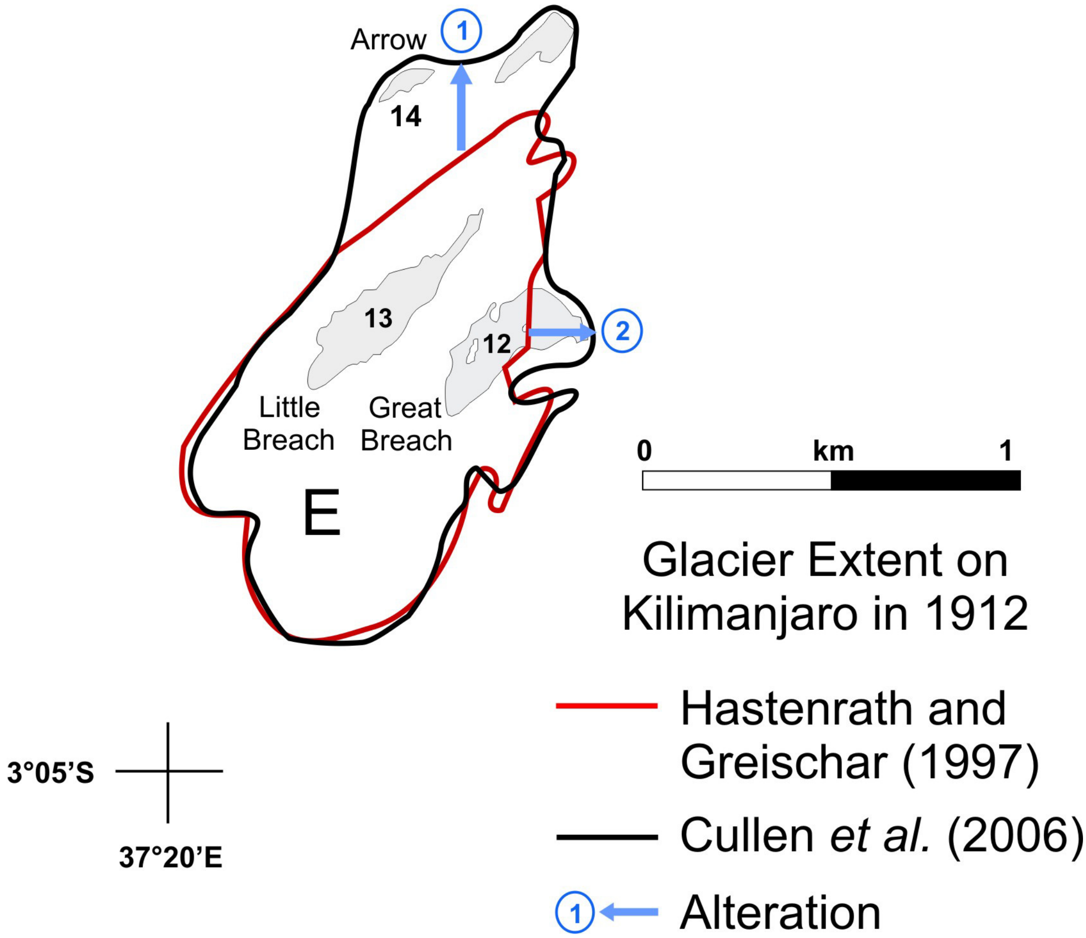

Fig. S4. Differences between outlines of ice in 1912 from Hastenrath and Greischar (3) and Cullen et al. (1). The two most prominent alterations in shape and extent are shown (also see http://bprc.osu.edu/Icecore/KilimanjaroGlacierRetreat.html)

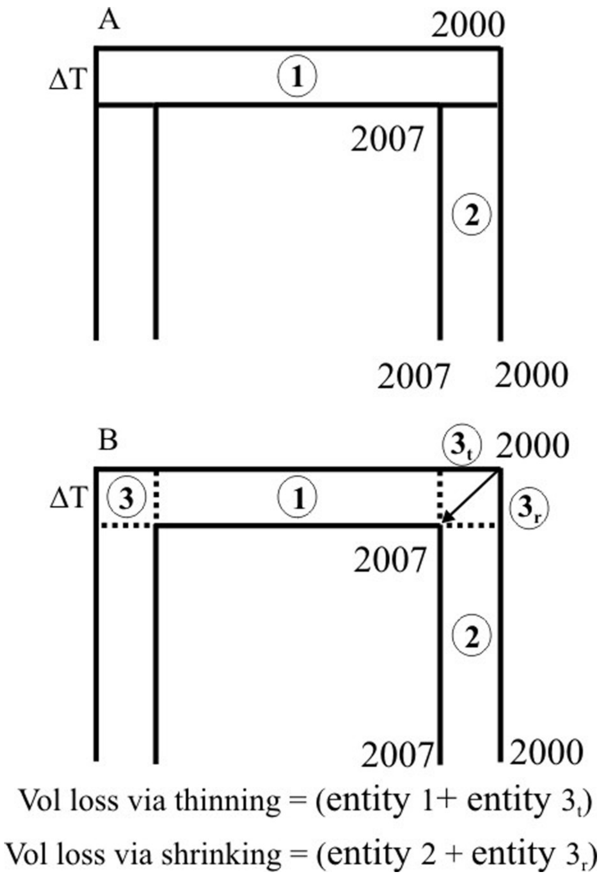

Fig. S5. Schematic showing ice loss calculation. The volume calculation described is shown in two dimensions (*x* and *z*) and is not to scale. The third dimension (*y*) is not shown. (*A*) Illustrates the calculated volume loss caused by thinning (entity 1) and that caused by shrinking (the sum of all entity 2s around the ice field as described). (*B*) Illustrates the adjustment required to entities 1 and 2 in light of the fact that the volume loss in entity 3 results from both thinning and shrinking.

Table S1. Kilimanjaro ice areas (m^2) for the ice fields in each entity (A, D, E, F) as shown in Figure S2 for the 2000, 2006, and 2007 maps

Glacier name, number, or entity as appropriate	2000	2006	2007	Change (2000–2007) 7.7 years		
				Area	%	% yr^{-1}
NIF (total)	1,153,009	973,324	947,093	−205,916	−17.9	−2.3
Drygalski (no. 18)						
Credner (no. 19)						
Northern (no. 20)						
Eastern (no. 2)	190,555	107,706	90,303	−100,252	−52.6	−6.8
Uhlig (no. 15)	9,232	4,942	3,904	−5,328	−57.7	−7.5
Little Penck (no. 16)	101,129	76,408	60,416	−40,713	−40.3	−5.2
Entity A	1,453,925	1,162,380	1,101,716	−352,209	−24.2	−3.2
SIF (total)	740,656	575,879	573,181	−167,475	−22.6	−2.9
Southern (no. 4)						
Rebmann (no. 5)						
Decken (no. 6)						
Kersten (no. 7)						
Ratzel (no.3)	1,730	0	0	−1,730	−100.0	−16.7
Heim (no. 8)	93,061	66,444	62,136	−30,925	−33.2	−4.3
Diamond (no. 10)	76,214	50,251	56,502*	−19,712	−25.9	−3.4
Entity D	911,661	692,574	691,819	−219,842	−24.1	−3.1
Little Breach (no. 13) (Entity E)	93,210	34,656	22,708	−70,502	−75.6	−9.8
Furtwängler (no. 9) (Entity F)	57,149	40,224	35,024	−22,125	−38.7	−5.0
Plateau and west slopes (Entities A + F)	1,511,074	1,202,604	1,136,740	−374,334	−24.8	−3.2
South slopes (Entities D + E)	1,004,871	727,230	714,527	−290,344	−28.9	−3.8
Total	2,515,945	1,929,834	1,851,267	−664,678	−26.4	−3.4
Plateau only	770,057	625,263	596,463	−173,594	−22.5	−2.9

Changes in ice area, percentage ice cover, and percentage ice cover per year for the 2000 to 2007 interval are calculated.
*Questionable because of fresh snow cover.

Table S2. The areas of ice cover in 2003 interpolated from 2000 and 2006 OSU determinations are compared with those from *Cullen et al.* (1) and shown along with their percentage differences

	Domain				
Statistic	A	D	E	F	Total
OSU-Int, km^2	1309	0.803	0.064	0.049	2.224
CU06, km^2	1.304	1.025	0.132	0.049	2.510
Difference CU06 − OSU-Int, km^2	−0.005	0.222	0.068	0.000	0.286
% Difference relative to OSU-Int	−0.38	27.7	106.3	0.0	12.9
% Difference relative to CU06	−0.38	21.7	51.5	0.0	11.4

Ice domains (A, D, E, and F) are as defined by Hastenrath and Greischar (3) and shown in Fig. S2. The difference between sum and total of first line is caused by rounding.

Table S3. Data used to calculate volume changes from 2000 to 2007 caused by surface lowering and area decrease for the NIF and FWG

Statistic	NIF	FWG
Area in 2000, m^2	1,153,000	57,100
Area in 2007, m^2	947,100	35,000
Change in area, m^2	205,900	22,100
Mean surface lowering, m	1.9	3.05
Volume loss by surface lowering, m^3; Fig. S5*A*, entity 1	2,190,700	174,300
Volume loss from area decrease, m^3, Fig. S5*A*, sum of all entity 2 s	1,869,200	146,900
Total volume loss (ΔVol), m^3	4,059,900	321,200
Volume of entity 3_r and 3_t in Fig. S5*B*, m^3	195,600	33,700
Adjusted volume loss by thinning, m^3	1,995,100	140,600
Adjusted volume loss by shrinking, m^3	2,064,900	180,700
$\Delta Vol_{lowering}/\Delta Vol_{shrinking}$	0.97	0.78
$\Delta Vol_{owering}/\Delta Vol_{total}$	0.49	0.44
$\Delta Vol_{shrinking}/\Delta Vol_{total}$	0.51	0.56

Area and volume data were rounded to the nearest 100 m^2 or m^3, respectively. The results indicate that ice field shrinking and lowering are contributing nearly equally to the volume loss on both NIF and FWG.